Combustion Kinetics of Char Obtained by Flash Pyrolysis of Pine Wood

Arthur M. C. Janse,[†] Harald G. de Jonge,[‡] Wolter Prins, and Wim P. M. van Swaaij*

Department of Chemical Technology, Twente University, P.O. Box 217, 7500 AE Enschede, The Netherlands

The combustion kinetics of rapidly pyrolyzed wood have been investigated within the temperature range of 573−773 K and the oxygen concentration range of 2.25−36 vol %. These kinetics are, for instance, required for the design of a char combustion section in an integrated flash pyrolysis pilot plant. Two different experimental techniques were used: a standard thermogravimetrical technique (TGA) and flue gas analysis after combustion in a diluted packed bed. The pyrolysis char was prepared in a small screen heater reactor, enabling heating rates of over 300 K/s. The results of the TGA and the packed-bed measurements are in good agreement for temperatures above 648 K. Below that temperature, the reaction rate observed in the TGA appears to be (up to 1.5 times) lower than that in the packed-bed reactor. The combustion kinetics can be described by the following simple rate equation which has an average deviation of 20%: $r = 5.3 \times 10^5 e^{-125\times10^3/RT} P_{O_2}^{0.53}(1 - X)^{0.49}$. Several pore models reported in the literature were tested against the experimental data, but they could not improve the accuracy of the fit. In comparison with available data, this specific type of char shows a notably higher rate of combustion.

1. Introduction

Because of a growing concern about the environment, research to the utilization of relatively clean and renewable energy sources such as biomass was much intensified during the last 2 decades. Not only has the direct generation of electricity from renewable energy carriers been considered but also the production of intermediates, like liquid fuels, was investigated. They can be stored and transported, which enables the decoupling of the biomass feedstock supply from the electricity generation process. Biomass-derived liquids can be obtained by flash pyrolysis, that is, fast thermal decomposition of ground carbonaceous material at 400−600 °C in the absence of an oxidizing agent. Char and gas are formed as byproducts; they can be used for generation of the heat required for the endothermic pyrolysis reactions in integrated combustion sections. Conversion of biomass to bio-oil includes a significant (energy) densification. Storage and transport of bio-oil is much easier than that for the bulky biomass. It can be applied as a fuel for engines or oil-fired boilers but also as a feedstock for the synthesis of valuable chemicals. Various types of flash pyrolysis processes have been developed. An excellent review is provided by Bridgwater and Bridge (1991). Emerging technologies use a fluid bed (Scott and Piskorz, 1982) or circulating fluid bed (Graham et al., 1988) as the pyrolysis reactor. During the last 5 years rotating-cone technology has been the subject of intensive research at Twente University (Wagenaar et al., 1994). Meanwhile, a 50 kg/h pilot plant has been built and delivered to Shenyang University in China. In succession to this prototype work, Twente University has continued its research and designed a strongly modified reactor with integrated heat generation and solids transport. Experiments with a new, small pilot plant are ongoing since Jan 1998; the results are quite good and will be published in due course. The core of this pilot plant, which is extensively described in a previous paper (Janse et al., 1996), consists of two reactor vessels. Flash pyrolysis takes place in the rotating-cone reactor, while the produced char is burnt in a fluid-bed combustor surrounding the rotating-cone reactor. The char combustion process is meant to deliver the heat to maintain the process. Operating temperatures of the rotating cone and the combustor are in the ranges 500−600 and 600−800 °C, respectively.

For the design of the combustor, the char combustion kinetics should be known. However, a lack of literature data exists concerning the combustion of wood char, especially for char which has been produced at high heating rates, like that in flash pyrolysis processes. The objective of this research is, therefore, to determine the oxidation kinetics of such wood char with two independent experimental techniques and to describe the kinetic data with a simple expression. Sawdust of pine wood has been used for this study because it is abundantly available and typically is used in flash pyrolysis processes.

It is generally impossible to determine intrinsic combustion kinetics at the high level of practical combustion. That would result in mass/heat-transfer controlled conditions for the laboratory equipment of the kinetic measurements, and the results would reflect the hydrodynamics of that specific piece of equipment instead of the true combustion rate. It is common practice to extrapolate the kinetic expressions derived at a lower temperature than the desired high-temperature level of practical combustors.

* Corresponding author. Telephone: 31-53-4892891. Fax: 31-53-4894774.

[†] Present address: Gist-Brocades, P.O. Box 1, 2600 MA Delft, The Netherlands. E-mail: arthur.janse@gist-brocades.infonet.com.

[‡] Present address: ATO-DLO, P.O. Box 17, 6700 AA Wageningen, The Netherlands.

S0888-5885(97)00705-7 CCC: $15.00
Published on Web 09/12/1998

Table 1. Literature Data for the Combustion Kinetics of Wood Char

	type of material	T_{pyr} (°C)	$(dT/dt)_{pyr}$ (°C/min)	T_r (°C)	conc. O_2 (%)	E_A (kJ/mol)	n	m
McCarthy (1981)	wood	720	20	370−452	21	152		0
Burggraaf et al. (1983)	wood		slow	312−446	5−20	131.5	0.87	0
Magnaterra et al. (1989)	hardwood	610	3	350−440	5−18	108.7	0.92	0
Kashiwagi and Nambu (1992)	cellulose	550	1−5	400−550	0.28−5.2	160	0.78	1
Magnaterra et al. (1992)	hardwood	610	3	350−480	2−18	84.9	0.74	$f(X)$[a]

[a] Conversion function of the complex pore model.

2. Literature

Although the amount of literature dealing with the combustion of coal and coal char is overwhelming, research concerning the combustion of wood char has hardly been carried out. The few available literature data are summarized in Table 1 and presented together with the related combustion conditions, viz., the temperature (T_r) and oxygen concentration (concentrated O_2). Because the char preparation (pyrolysis) conditions can have a strong influence on its chemical composition and pore size distribution (see, for example, Laurendeau, 1978), also the most important pyrolysis conditions, such as the heating rate of the wood sample $(dT/dt)_{pyr}$ and the pyrolysis temperature (T_{pyr}), are listed. Finally, the type of feedstock and the reported kinetic parameters are indicated. These kinetic parameters belong to the following simple homogeneous rate equation, in which a particle is represented as a uniform nonporous grain:

$$r = k_0^{-E_A/RT} P_{O_2}^{\ n} (1 - X)^m \qquad (1)$$

The table shows a wide variety in results, which are caused by the differences in feedstocks, char-preparation conditions, and experimental methods. Experiments to obtain kinetic data above 500 °C can be disturbed by heat- and/or mass-transfer limitations. For coal char, the influence of pyrolysis process conditions on the combustion kinetics is much more established than that for wood char. In the following subsection, we will briefly summarize what is known with respect to coal char.

2.1. Effect of Preparation (Pyrolysis) Conditions on Coal Char Reactivity. Several authors (Kristiansen, 1995; Hindmarsh et al., 1995; McDonald et al., 1992; Miura et al., 1989; Patel et al., 1988; Zygourakis, 1988; Radovic et al., 1983; Jenkins et al., 1973) show that the combustion kinetics of coal char are influenced markedly by the heating rate of the initial coal sample, the residence time at the final pyrolysis conditions, the applied final pyrolysis temperature, and the presence of inorganics in the coal (and char) sample.

Hindmarsh et al. (1995) performed the pyrolysis of coal in a wire-mesh reactor (also indicated as a screen heater reactor) and in an entrained-flow reactor (drop tube). A relatively strong effect of the pyrolysis temperature on the char reactivity was observed; it decreased by a factor of 20 over the T_{py} range of 923−1173 K. The holding time was found to be unimportant, but the char reactivity increased by a factor of 4 when the heating rate of the sample was raised from 2 to 5000 K/s. Work of Jenkins et al. (1973) shows that increasing the pyrolysis temperature from 873 to 1173 K decreases the reactivity by a factor 3.

Zygourakis (1988) found that for lignite, a low-rank coal type which perhaps can be best compared to wood, the porosity and surface area are only slightly enlarged when the heating rate is increased from 0.1 to 1000 K/s. Similarly, McDonald et al. (1992) concluded that the surface area is not so much affected by the heating rate or pyrolysis temperature. They found instead that the H/C ratio of the char is influenced notably by both parameters. This H/C ratio increases with increasing heating rate but decreases when the final pyrolysis temperature is elevated.

Miura et al. (1989) deduced from their experiments that the reactivity of low-rank coals (with less than 80 wt % C) is mainly determined by the presence of catalytically active metals like Ca, Fe, Na, and K, while for high-rank coals, it is controlled by the intrinsic reactivity.

In a recent review on coal pyrolysis, Kristiansen (1995) concluded that if the severity of the pyrolysis process increases (implying higher pyrolysis temperatures, longer holding times, and lower heating rates), the reactivity of the produced char decreases. The effect of a low heating rate, however, is not caused by a substantial decrease of reactive surface area but rather by a more pronounced formation of aromatic and graphite-like compounds, which arecharacterized by a low H/C ratio (McDonald et al., 1992). Another consequence of low heating rates may be a decreased dispersion of catalytic metal oxides. This would also reduce the reactivity of the produced char.

On the basis of the above literature results for coal-derived char combustion, it can be expected that also the process conditions during flash pyrolysis of wood are very important for the combustion properties of the simultaneously produced char. With respect to the available literature results on wood char combustion kinetics (Table 1), one should realize that the chars considered were produced while applying quite low heating rates. In flash pyrolysis of wood, the char is produced at heating rates which are much higher (up to 1000 K/s). Small particles (d_p < 1−2 mm) are used then to reduce the internal heat transport limitation, while the external heat-transfer rate is maximized by selection of appropriate reactor conditions. The high heating rates are essential and should be taken into account when the combustion behavior of char produced in flash pyrolysis processes is studied.

2.2. Reaction Mechanism. The models applied to describe the kinetic data generally result in a rate equation of the following form:

$$r = k_0 e^{-E_A/RT} P_{O_2}^{\ n} \frac{S(X)}{S_0} \qquad (2)$$

where the last term, $S(X)/S_0$, represents the relative change in available surface area during the reaction. The conversion X is defined as

$$X = \frac{M_0 - M(t)}{M_0 - M_\infty} \tag{3}$$

in which M_0 is the initial char mass, $M(t)$ the mass after a certain reaction time t, and M_∞ the mass after infinite reaction time (the mass of remaining ash).

From a fundamental mechanistic point of view the reaction order with respect to oxygen should be in the range between 0 and 1 (Laurendeau, 1978; Lin et al., 1991). At high temperatures (>700−800 °C) the order tends to the value 1, and for low temperatures (300−400 °C), it tends to the value 0. This can be explained by the following reaction mechanism:

$$2C + O_2 \rightarrow 2C(O) \tag{R1}$$

$$C(O) \rightarrow CO \tag{R2}$$

$$C(O) + C(O) \rightarrow CO_2 + C \tag{R3}$$

(R1) represents the chemisorption of oxygen on two active sites, and (R2) and (R3) represent the formation of CO and CO_2, respectively, through desorption and surface reaction. It can be expected that the reaction order with respect to oxygen will be 1 when (R1) is the rate-determining step. When (R2) and (R3) are rate-determining, zero-order dependency will be found. Usually, (R1) competes with (R2) and (R3) and an order between 0 and 1 will be found. At low reaction temperatures, (R2) and (R3) will be rate-determining.

2.3. Combustion Models. In the past, several pore models have been developed to describe the development of the internal surface of a pyrolyzing wood particle ($S(X)/S_0$). An overview of the various pore models is presented by Weeda (1995). He divided them into three distinct different classes: grain, capillary, and discrete models. The first class describes the pore structure of a char particle as consisting of a group of spherical grains. The void between these grains are considered to represent the macroporosity, while the micropores are formed by the void inside the grains. Capillary models describe the pore structure as a collection of capillaries or spherical cavities with different sizes. As the reaction proceeds, the size of the capillaries or cavities increases, also by the coalescence of the growing pores. Discrete models put cavities randomly on a discrete grid and let the cavities grow according to the reaction rate.

In this work, it is also attempted to apply a (pore) model from the literature for the description of the experimentally determined kinetic data. Therefore, besides the homogeneous model (eq 1), which represents a particle as consisting of one phase, a few (capillary) pore models have been selected based on simplicity (final model equation), number of adjustable (fit) parameters, and physical meaning. Table 2 presents the models considered with their essential input parameters. $S(X)/S_0$ describes the development of the pore surface area with respect to the area initially present as a function of the conversion X.

The model equations of Bhatia and Perlmutter (1980), Gavalas (1980), and Tseng and Edgar (1989) have the same mathematical form and will therefore show the same accuracy in predicting kinetic data. In contrast with the model of Simons and Finson (1979), the fit parameters cannot be determined a priori from initial structure data. Chars sometimes show a maximum in reaction rate with increasing conversion X, which is attributed to an increasing and subsequently decreasing pore surface area (caused by the coalescence of growing pores). All of the presented model equations, except the power-law model, predict a maximum in the reaction rate as a function of the conversion. The way in which this maximum is affected by the combustion temperature (section 5.2) is not included in the equations of Table 2.

3. Preparation of Wood Char

The literature dealing with combustion of coal char indicates that preparation conditions like the pyrolysis temperature and heating rate influence the combustion kinetics strongly. The wood char of this work has been prepared under conditions similar to those at which the rotating-cone reactor is operated. This could be realized by applying a so-called "screen heater reactor" (Westerhout et al., 1998), in which heating rates up to 10 000 K/s can be achieved. A schematic drawing of the reactor is depicted in Figure 1.

The reactor consists of two wire gauzes which are clasped between two electrodes. A thin plate of fine, compacted particles is prepared by drying a suspension of pine-wood powder in water. This wood powder, with an average particle diameter of 90 μm (80−106 μm), was obtained by grinding of coarser material (1−3 mm diameter) in a hammer-mill. The pine-wood plate, having a width of 5 mm, a length of 15 mm, and a thickness of 0.7 mm, is placed on the screen. At the beginning of an experiment, the equipment (and also the sample) is first heated to 150 °C under nitrogen, to avoid condensation of tars (and fouling) of downstream pipings during the pyrolysis process. Subsequently, a very high current (60 A) is applied to the screen. As a consequence, the wood sample is heated very rapidly to the desired pyrolysis temperature (600 °C). The temperature is then kept at a constant value for 60 s, after which the sample is cooled under nitrogen to room temperature. The char is subsequently scraped from the screen and collected in a small bottle, in which it is stored (in air at room temperature) until utilization. It has been checked extensively that the storage time (maximal 3 weeks in air) had no influence on the combustion characteristics of the sample.

From an initial wood mass of 100 mg, 5 mg of char could be produced. Although the heating rate of the screen itself is extremely high, the center of the little sawdust plate is heated less rapidly due to heat penetration limitation. Nevertheless, Fourier calculations showed that the heating rate in the center of the plate is still (at least) 300 K/s, which is of the same order as experienced by wood particles in the rotating-cone reactor.

The three most important variables in the char production process are (1) the heating rate (determined by the thickness of the wood plate), (2) the final pyrolysis temperature, and (3) the pyrolysis time, or the period during which the sample is kept at the final pyrolysis temperature. A number of separate experiments have been carried out to elucidate the influence of these variables. Results of these experiments are discussed in section 5.1.

4. Experimental Conditions

The combustion experiments have been carried out in two different setups. In the first place, a standard

Table 2. Pore Models (Weeda, 1995) Tested against the Experimental Results

pore model	model equation	param
power-law (grain) model (Kristiansen, 1995)	$\frac{S(X)}{S_0} = (1-X)^n$	n: no physical meaning
pore tree model (Simons and Finson, 1979)	$\frac{S(X)}{S_0} = (1-X)\sqrt{\frac{X}{\epsilon_0} + (1-X)}$	ϵ_0: initial porosity
random pore model (Bhatia and Perlmutter, 1980)	$\frac{S(X)}{S_0} = (1-X)\sqrt{1 - \varphi \ln(1-X)}$	φ: structure parameter
random capillary model (Gavalas, 1980)	$\frac{S(X)}{S_0} = (1-X)\sqrt{1 - \frac{B_0}{2\pi {B_1}^2}\ln(1-X)}$	B_0: total pore length. B_1: total pore surface
bifurcated pore model (Tseng and Edgar, 1989)	$\frac{S(X)}{S_0} = (1-X)\sqrt{1 - \frac{1}{\ln\left(\frac{1}{1-\epsilon_{\text{micropore},0}}\right)}\ln(1-X)}$	$\epsilon_{\text{micropore},0}$: initial micropore porosity

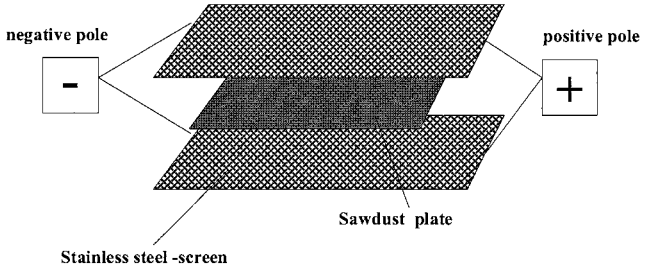

Figure 1. Schematic picture of the screen heater reactor.

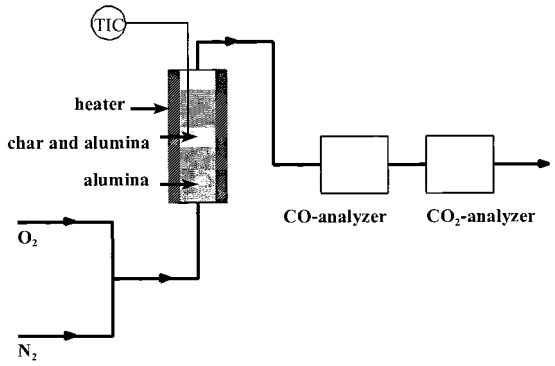

Figure 2. Flow sheet of the packed-bed equipment.

thermogravimetric analysis (TGA) apparatus has been used (Cahn 2000 system; accuracy of 10^{-6} g). An extensive description of this well-known and widely used equipment is, for instance, presented by Wigmans et al. (1983). Because of the risk of undesired mass- and heat-transfer limitations, the TGA is not applicable at high temperatures. In a diluted packed-bed reactor, somewhat higher temperatures can be applied because of the higher heat- and mass-transfer rates. An additional advantage of using two experimental techniques is the possibility of comparing the kinetic data obtained with different techniques over the possible range of equal reaction conditions.

Thermogravimetric Analysis Method. A certain amount of cold char (typically 0.3−0.4 mg) was put into the small sample basket of the TGA. At the start of an experiment, the hot tube furnace was positioned quickly around the sample holder, after which the weight decrease in time was recorded. The temperaturewas recorded by a thermocouple positioned 1 mm below the sample basket.

Preliminary experiments revealed that very high reaction rates occur if compared to literature data. Therefore, only very small amounts of char could be used to avoid an unacceptable temperature increase of the sample. Experiments (at 400 °C and 18% O_2) with a very thin 0.1-mm-diameter thermocouple close to the char surface showed that the temperature rise of a 4.5-mg char sample was approximately 80 K. When the sample size was decreased to 2.5 mg, the temperature increase dropped to 30 K. In the case of a 1-mg char sample, the maximum temperature increase was only 7 K. On the basis of this experience, char samples used in the experimental work were always kept smaller than 0.5 mg to avoid a significant temperature increase. Theoretical calculations (see the appendix) also indicate a maximum temperature rise of at most a few degrees for such small samples.

It has also been verified experimentally and theoretically that mass-transfer limitations are excluded. For instance, no difference in the burn-off curve was observed when the nitrogen of the gas mixture was replaced by helium, in which oxygen has a 5 times higher diffusion coefficient. Besides, a conservative calculation on the basis of $Sh_{\text{basket}} = 2$ showed that, even at the highest measured reaction rate, sufficient oxygen could be transported to the char surface by diffusion alone.

A gas flow of 250 NmL/min was applied for all measurements, corresponding to a gas velocity through the hot tube of approximately 5 cm/s. The gas consisted of a mixture of air and nitrogen, except for the highest oxygen concentration when pure oxygen and nitrogen were mixed to the specified ratio and supplied to the furnace tube. Combustion experiments have been carried out within a temperature range of 300−450 °C and an oxygen concentration range of 2.25−36 vol %.

Packed-Bed Equipment. A small-diameter (2-cm) packed bed has been used as a second experimental technique. A flow sheet of the experimental setup is shown in Figure 2. The bed is divided into three different zones: two layers of inert γ-alumina (mean diameter 65 μm) at the top (1.5 cm) and bottom (3 cm) with a mixture of 1−5 mg of char in 5 g of alumina (1.5 cm) between them. A thermocouple was inserted into the reaction zone, and it has been verified by repositioning that the temperature in the reaction zone was uniform (the fraction char must be low enough to avoid local temperature gradients). Extensive experiments have been carried out to ensure that the total temperature increase of the bed remained within 3 K during a combustion experiment. The size of the char sample has been varied from 1 to 10 mg, depending on the rate of reaction, to realize detectable CO and CO_2 concentration levels in the off-gas stream. Theoretical calcula-

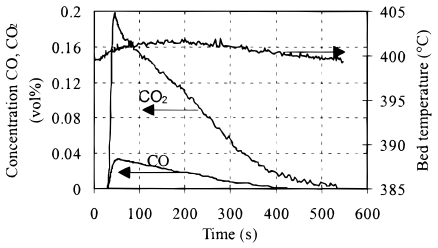

Figure 3. Time-dependent CO_2, CO, and temperature profiles during a packed-bed combustion experiment.

Table 3. Elemental Composition of Sawdust and Char

	sawdust (wt %)	char (wt %)
C	47.0	76.0
H	6.3	2.4
O	46.4	13.5
N	0.0	1.1
ash	0.3	7.0

Table 4. Ash Composition

	wt %
CaO	72
K_2O	9
MgO	8
SO_3	5
MnO	4
SiO_2	2

tions (see the appendix) indicate that the temperature increase of the sample should be less than 7 K.

At the beginning of an experiment, the bed was heated to the desired reactor temperature in an inert atmosphere of nitrogen. Then, the gas flow was switched to a mixture of air (or oxygen in the case of a desired oxygen concentration of 36 vol %) and nitrogen (300 NmL/min). The outlet concentrations of CO and CO_2 were measured continuously with (Mayhak) infrared CO and CO_2 analyzers. Transient concentration profiles could be derived after correction for the distribution in residence time in the packed bed, piping, and analyzers. The residence time distribution function has been determined from the response on a step disturbance in the concentration level of a CO_2-containing nitrogen flow through the system (Prins, 1987). An example of the results is presented in Figure 3, which also shows the observed temperature in the center of the bed.

When the initial carbon content of the char was recalculated from the measured CO_2 and CO concentration profiles, the percentage was always found to be between 70 and 80 wt %, which corresponds to the analytically determined value (see Table 3). Further, the replacement of the alumina particles by sand had no influence on the burn-off curve of the char, which means that alumina does not catalyze the combustion reactions if the sand is assumed to be inert. The packed-bed combustion experiments have been carried out within a temperature range of 350−500 °C and an oxygen concentration range of 2.25−36 vol %.

The chemical composition of both the pine wood and the derived char is presented in Table 3,while Table 4 shows the ash composition. The mean diameter of the char particles, as determined by infrared analysis is 89 μm. A rather low value (Laurendeau, 1978) of the BET surface area was found (178 m^2/g of char). This may be due to the liquidlike behavior of wood during the flash pyrolysis process, which hampers the formation of many small cavities and the corresponding creation of a large surface area.

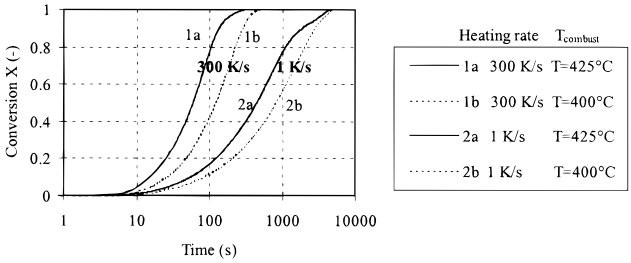

Figure 4. Influence of the heating rate on the burn-off curve (recorded for the packed-bed reactor at an oxygen concentration of 18 vol %). Char preparation conditions: pyrolysis temperature, 600 °C; holding time at 300 K/s, 60 s; holding time at 1 K/s, 375 s.

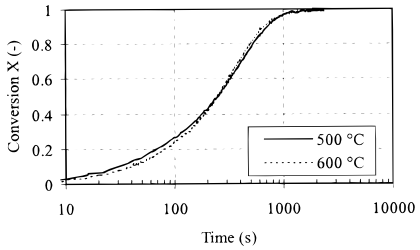

Figure 5. Influence of the pyrolysis temperature on the char burn-off curve (recorded for the TGA at a combustion temperature of 300 °C and an oxygen concentration of 18 vol %). Char preparation conditions: heating rate, 300 K/s; pyrolysis time, 20 s.

5. Results

5.1. Influence of Char Preparation (Pyrolysis) Conditions. As explained in section 3, the wood char whose combustion kinetics are to be determined has been prepared by pyrolysis in a screen heater setup. The influence of the pyrolysis conditions on the char combustion kinetics are now discussed. With respect to the effect of the adjusted heating rate, Figure 4 shows the (dimensionless) conversion versus time curve (also indicated as the burn-off curve) of char samples prepared at a pyrolysis temperature of 600 °C and heating rates of 1 and 300 K/s, respectively (estimates). The curve indicated with the 300 K/s heating rate label refers to char prepared in the screen heater reactor. The 1 K/s curve represents a char sample prepared in the packed bed (PB); such a low heating rate could not be realized in the screen heater reactor. The burn-off curves shown in the figure have been derived from combustion experiments in the packed-bed reactor. It can be concluded that high heating rates yield a highly reactive char; the reaction time is decreased by nearly an order of magnitude upon changing the heating rate from 1 to 300 K/s.

The influence of the applied final pyrolysis temperature is depicted in Figure 5 which shows the TGA burn-off curves of char samples prepared in the screen heater at a temperature of 500 and 600 °C, a pyrolysis time of 20 s, and a heating rate of at least 300 K/s. These two char preparation temperatures represent the limits between which the future rotating-cone reactor for flash pyrolysis of biomass will be operated. The result of the experiment presented in Figure 5 is quite remarkable, because it was expected that when the severity of the pyrolysis process increases, the reactivity of the produced char would decrease. It seems that theheating rate is decisive, while the final pyrolysis temperature is of minor importance in the range of 500−600 °C.

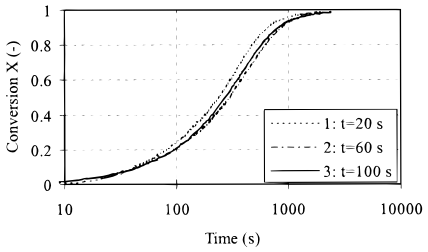

Figure 6. Influence of the pyrolysis time on the char burn-off curve (recorded for the TGA at a combustion temperature of 300 °C and an oxygen concentration of 18 vol %). Char preparation conditions: heating rate, 300 K/s; pyrolysis temperature, 600 °C.

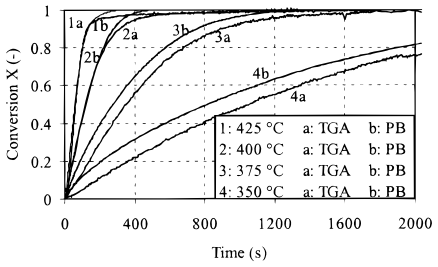

Figure 7. Comparison between TGA and packed-bed experiments (18 vol % O_2) in a conversion versus time plot and for different combustion temperatures.

Figure 6 illustrates the effect of the applied pyrolysis time for TGA measurements. Three different samples have been exposed to a final pyrolysis temperature of 600 °C for 20, 60, and 100 s. As can be seen, the differences are quite small. On the basis of the results shown in Figures 4−6, it has been decided to produce all of the char samples at the maximum heating rate of at least 300 K/s while keeping them for 60 s at a final pyrolysis temperature of 600 °C.

5.2. Combustion Results. A number of experiments in the TGA and the packed bed were carried out at the same process conditions, which allows a comparison of the two different techniques. An example of such a comparison is presented in Figure 7. This figure shows burn-off curves recorded for both the packed bed and the TGA, at four different temperatures but always the same oxygen concentration (18 vol %).

The agreement of the results is quite good at temperatures of 400 and 425 °C but becomes worse at 375 and especially 350 °C. Generally, the difference between the two techniques increases at lower temperatures, where the observed reaction rate in the packed bed is higher than that in the TGA. Perhaps the adsorption of oxygen on the char surface (especially at lower temperatures) can influence the measured weight decrease in time notably (Floess et al., 1988). Oxygen adsorption may cause the measured burn-off rate in the TGA to be lower than that in the packed bed equipment. Also the work of Brown et al. (1992), who studied the chemisorption of oxygen on carbon (Spherocarb) between 420 and 920 K, indicated that the formation of stable surface oxide complexes can disturb weight loss measurements in a TGA.

Literature data on the combustion of coal char show that the reaction rate can pass through a maximum at 20−30% conversion (see, for instance, Tseng and Edgar, 1985). At low conversion, growth of pores causes an increase of the internal surface area. However, this process stops when the pores become so large that coalescence must occur. Beyond 20−30% conversion, the effect of pore coalescence is dominant and the

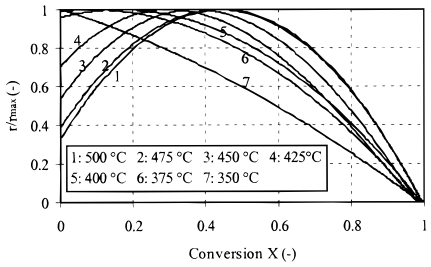

Figure 8. Dimensionless reaction rate as a function of the conversion, for various combustion temperatures (packed bed, at an oxygen concentration of 9 vol %).

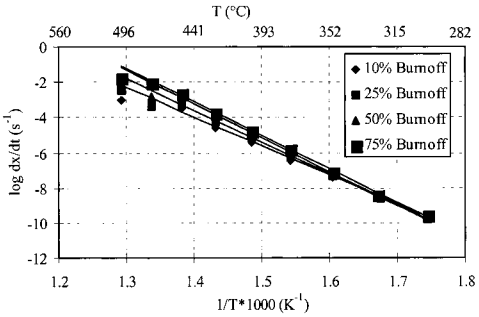

Figure 9. Example of an Arrhenius plot at four different conversions (recorded in the TGA at an oxygen concentration of 18 vol %).

internal surface area will decrease continuously. This phenomenon has been observed at all temperatures above 350−375 °C, but it depends on the type of coal.

Figure 8 shows results of this work as the determined reaction rate divided by the maximum reaction rate (r/r_{max}) for packed-bed measurements as a function of the conversion. Similar curves can be derived for any other oxygen concentration and both experimental techniques. At a temperature of 350 °C, the reaction rate decreases continuously, whereas at higher temperatures, a maximum is observed. Apart from the previously mentioned explanation concerning pore surface development, this effect can also be due to the competing reactions of adsorption (reaction (R1)) and desorption (reactions (R2) and (R3)). The adsorption step is known to be slow with respect to the gasification rate (desorption step) at moderate (400−500 °C) temperatures (Floess et al., 1988). However, at 350 °C the adsorption step is still fast enough to keep up with the desorption reactions, but at higher temperatures, the adsorption becomes rate limiting. First, a layer of oxygen−carbon complexes will be formed slowly on the surface, after which the reaction can proceed. This may also explain the S-shape of the burn-off curves at high temperatures.

The overall activation energy of the combustion reaction can be obtained by plotting the logarithmic conversion rate $\ln(dX/dt)$ versus the inverse temperature $1/T$ (also called an Arrhenius plot, see (1)). The slope of the curve equals $-E_A/R$. An example of an Arrhenius plot is presented in Figure 9, in which the reaction rate is depicted as determined from TGA experiments at an oxygen concentration of 18 vol %. Although in this figure measurements up to 500 °C are presented, TGA data for temperatures above 450 °C have been rejected as input for the kinetic expression parameter estimation to exclude any influence of possible mass-transfer limitations. It can be observed from Figure 9 that, especially at temperatures above 450 °C, the slope of the curves decreases. This is an indication for the occurrence of mass-transfer limitation.

Table 5. Activation Energy for Various Conversion Levels (X) and Oxygen Concentrations (TGA)

	E_A (kJ/mol)			
% O_2	$X = 0.1$	$X = 0.25$	$X = 0.5$	$X = 0.75$
2.25	108.6	116.6	121.4	114.3
4.5	111.1	131.7	142.0	144.3
9.0	126.7	137.4	146.6	148.7
18.0	137.2	150.2	154.4	159.0
36.0	137.2	151.7	160.9	152.1
overall	115.2	129.1	139.3	139.9

Table 6. Activation Energy for Various Conversion Levels (X) and Oxygen Concentrations (Packed Bed)

	E_A (kJ/mol)			
% O_2	$X = 0.1$	$X = 0.25$	$X = 0.5$	$X = 0.75$
2.25	96.8	109.0	114.7	113.4
4.5	95.1	113.3	120.6	115.8
9.0	103.9	120.0	128.9	127.2
18.0	111.5	129.4	138.3	136.6
36.0	108.3	129.1	139.0	136.9
overall	103.2	122.2	128.3	125.9

In Tables 5 and 6 the derived activation energies are listed for both the TGA and the packed-bed (PB) measurements as a function of the oxygen concentration and for four different conversion levels. In these tables low conversions and low oxygen concentrations correspond with low values of the activation energy. At high oxygen concentrations and conversions theactivation energy reaches a constant value. The shifting value of E_A could be caused by a change in the reaction mechanism. As mentioned already, reaction (R1), the adsorption of oxygen on the char surface, competes with the desorption steps (R2) and (R3) at the temperatures of investigation. Apparently, the adsorption step becomes less important at higher oxygen partial pressures. This is in agreement with other literature: Laurendeau (1978) reported an activation energy for the adsorption step on the order of 80 kJ/mol (order in oxygen concentration equal to 1) while the desorption step has a much higher activation energy (on the order of 300 kJ/mol; the reaction order with respect to oxygen equals 0). He mentioned an activation energy of 120−150 kJ/mol for an intermediate reaction mechanism with an order in oxygen concentration of 0.5. The reported range of activation energies is in agreement with the values observed in this work. Also Lin et al. (1991), who studied the combustion kinetics of coked sand, gave the same range of values for the activation energy and the same trend of increasing activation energies with increasing oxygen partial pressures.

The order with respect to the oxygen concentration n can be determined by plotting the reaction rate r versus the oxygen concentration $\ln(P_{O_2})$. According to (2), for a constant temperature and conversion level, the slope of this curve is equal to n. Values of the order n derived from of the TGA and packed-bed experiments are listed in Tables 7 and 8, respectively. They show an increasing influence of the oxygen concentration on the reaction rate at increasing temperature for all four conversion levels included. As explained before in section 2.2, the rate-limiting step in the reaction mechanism changes from (R2) and (R3) (the desorption steps) to (R1) (the adsorption step) at increasing temperature. A second observation from Tables 7 and 8 is that the order in oxygen concentration decreases with increasing conversion, implying that (R1) becomes less important relative to (R2) and (R3). This is in agreement with Floess et al. (1988), who also explained this effect by a decreasing oxygen concentration on the surface.

Table 7. Reaction Order for Oxygen, Derived for Various Temperature and Conversion Levels (TGA)

	order in oxygen n			
temp (°C)	$X = 0.1$	$X = 0.25$	$X = 0.5$	$X = 0.75$
300	0.391	0.357	0.312	*a*
325	0.406	0.350	*a*	*a*
350	0.491	0.441	0.363	0.314
375	0.561	0.514	0.455	0.409
400	0.662	0.644	0.596	0.521
425	0.724	0.735	0.709	0.643

[a] Data have been rejected because of inaccurate measurement.

Table 8. Reaction Order for Oxygen, Derived for Various Temperature and Conversion Levels (Packed Bed)

	order in oxygen n			
temp (°C)	$X = 0.1$	$X = 0.25$	$X = 0.5$	$X = 0.75$
350	0.476	0.415	0.347	0.256
375	0.508	0.470	0.405	0.328
400	0.518	0.494	0.456	0.419
425	0.577	0.551	0.540	0.525
450	0.579	0.554	0.560	0.547
475	0.675	0.707	0.682	0.606
500	0.678	0.715	0.687	0.587

Our more or less mechanistic explanation on the basis of the reaction scheme presented in section 2.2 for the observed values of the activation energy and order in oxygen could be confirmed by determining the ratio CO/CO_2. This ratio should, for example, increase with increasing reaction temperature according to the current interpretation of the experimental results. However, over the investigated temperature and oxygen range, there is a nearly constant value between 0.15 and 0.2. This result is in contradiction with the observation of other authors (see, for example, Laurendeau, 1978; Ismael and Walker, 1989), who reported always increasing ratios at higher temperatures. In this work, the range of investigated temperatures has perhaps been too small for a decisive conclusion. The constant CO/CO_2 ratio would imply that the activation energies for (1) and (2) are nearly equal. It has been verified that secondary CO oxidation reaction in piping and analyzers could be neglected. This was done by measuring the temperature at a distance of approximately 1 cm from the reactor outlet. The temperature of the flue gas appeared to be dropped at this point to nearly room temperature, which excludes oxidation of CO in secondary equipment.

The pore models presented in Table 2 have been fitted to the data of both the TGA and packed-bed measurements. As a result, values of the pre-exponential factor k_0, the activation energy E_A, and the order with respect to oxygen n could be derived. Apart from these kinetic parameters, also the correlation coefficient r^2, which is a measure of the correctness of the fit, was obtained. The fit has been carried out by dividing the recorded burn-off curve for each temperature and oxygen concentration (both for the packed bed and the TGA) in 10 equal conversion parts to be sure that the final rate equation can describe the whole conversion range. The fit parameters of the several models have been adjusted using the least-squares method, until the difference between the experimental and calculated time to reach a certain conversion (10, 20, 30, ..., 90%) was minimized.

Table 9. Comparison of Five Literature Models for Wood Char Combustion Kinetics

model	k_0 (s^{-1})	E_A (kJ/mol)	n	pore structure parameter	r^2
homogeneous rate equation (1)	1.064×10^5	124.8	0.529	$m = 0.487$	0.941
Simons and Finson (1979)	2.332×10^5	125.0	0.530	$\epsilon_0 = 0.160$	0.950
Bhatia and Perlmutter (1980)	4.434×10^5	124.9	0.529	$B_0 = 5.323 \times 10^{-3}$ $B_1 = 1.778 \times 10^{-2}$	0.943
Gavalas (1980)	4.434×10^5	124.9	0.529	$\psi = 2.679$	0.943
Tseng and Edgar (1989)	4.434×10^5	124.9	0.529	$\epsilon_{micropore,0} = 0.687$	0.943

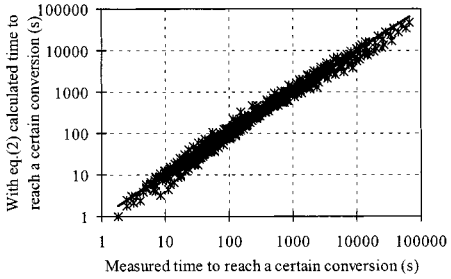

Figure 10. Parity plot in which combustion times for 10 different conversion levels, and for all TGA and packed-bed samples, are compared with the ones calculatedfrom (1) (average deviation 20%).

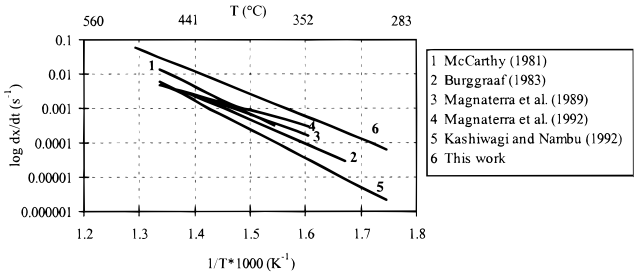

Figure 11. Arrhenius plot (reaction rate versus temperature) of the best fit rate equation of this work and other literature data.

From Table 9 it can be concluded that the various pore models presented in the literature do not give a substantially better description of the kinetic data of our measurements than the simple homogeneous model. The unrealistic low value of ϵ_0, representing the initial porosity in the pore model of Simons and Finson, implies that this model is not well-suited for the description of the combustion behavior of this char. A parity plot illustrating the accuracy of the homogeneous model is presented in Figure 10. This shows the conversion time calculated with the model versus the experimentally observed conversion time. The conclusion is justified that the homogeneous model describes the kinetic data with sufficient accuracy.

It is now interesting to compare our "best fit" kinetic rate equation with other (homogeneous) rate correlations for the combustion of wood char. The belonging kinetic parameters (of eq 1) are listed in Table 1. Figure 11 shows the result of this comparison in a single Arrhenius plot.

It must be emphasized that any of the correlations presented should only be applied in the original range of investigation; that is why the lengths of the correlation lines in Figure 11 vary.

The comparison shows that the wood char produced for this work has a much higher reactivity, up to 1 order of magnitude, than the chars considered in the literature. Probably, the high heating rate applied in the present study results in a relatively high H/C ratio of the char. To clarify the influence of minerals, a number of separate experiments have been carried out with char that was treated with a 5 M HCl solution for 2.5 h at 50 °C. This treatment induced a lower Ca content in the char (50% decrease) but an increased level of Cl (10-fold increase). The char reactivity decreased by a factor 3−4, which illustrates that the effect of catalytic metals can be quite significant. This is especially important for chars obtained by flash pyrolysis processes, which produce only small amounts of char. As a consequence, the mineral content can be quite high.

Unfortunately, it cannot be excluded completely that the electrical current applied in the screen heater has some influence on the chemical structure of the produced char. Recently, Shevchenko et al. (1993) showed that an alternating electric current can influence the reaction rate during steam gasification which was attributed to the formation of a hot plasma in the micropores, due to electric discharge. In our combustion experiments no current was applied, but further investigations should be carried out to clarify any possible influence of the screen current during the preparation.

Finally, the screen heater setup was not equipped with a variable heating rate device which would have allowed the application of a whole range of heating rates. Future investigations are needed to determine the precise effect of the heating rate during the char production step.

6. Conclusions

Wood char has been prepared in a screen heater reactor by pyrolysis under nitrogen at a heating rate of at least 300 K/s. The influence of pyrolysis process variables such as the pyrolysis time and temperature has been investigated. At pyrolysis times of 20−100 s, no influence of this parameter on the char reactivity could be observed. The difference in reaction rates of char prepared at 500 and 600 °C (the process conditions of the continuous pyrolysis plant) appeared to be minor.

Two experimental techniques have been applied to determine the combustion kinetics of the produced char: a TGA and a diluted-bed off-gas analysis method. The range of investigated temperatures was between 573 and 773 K, while the oxygen concentration was varied between 2.25 and 36 vol %. Above 375 °C, the agreement between the results of both techniques is quite good, but it becomes worse at lower temperatures. This might be caused by the adsorption of oxygen on the surface, which results in a slower weight decrease of theTGA sample. Although several pore models from the literature have been tested, a simple, homogeneous (power-law) model was sufficient to give an accurate description of the observed kinetics:

$$r = 5.3 \times 10^5 e^{-125 \times 10^3/RT} P_{O_2}^{0.53} (1 - X)^{0.49} \qquad (4)$$

The wood char produced in this work has a much higher reactivity, up to 1 order of magnitude, than the wood chars considered in the literature.

Acknowledgment

This investigation was supported by the CEC-AIR program (AIR-Contract CT93-0889). We also acknowledge J. Nijmeijer, J. Waanders, and G. Schorfhaar for their assistance in the experimental work.

Symbols

B_0, B_1 = pore structure parameters in the pore model of Gavalas (1980)
E_A = activation energy [kJ/mol]
k_0 = pre-exponential factor [l/s]
n = reaction order with respect to oxygen
m = reaction order with respect to unconverted char
M_0 = initial mass [kg]
M_∞ = mass after infinite reaction time [kg]
$M(t)$ = mass [kg]
P_{O_2} = partial oxygen pressure [Pa]
r = rate of reaction [kg/(kg/s)]
R = gas constant [J/(mol/K)]
S = surface area [m^2]
S_0 = initial surface area [m^2]
T = temperature [K]
T_{pyr} = pyrolysis temperature [K]
T_r = reaction temperature [K]
X = conversion

Greek Letters

ϵ = porosity
ϵ_0 = initial porosity
$\epsilon_{micropore,0}$ = initial micropore porosity (pore model of Tseng and Edgar (1989))
φ = pore structure parameter in the model of Bhatia and Perlmutter (1980)
ψ = pore structure parameter in the model of Gavalas (1980)

Appendix: Validation of the Absence of Heat-Transfer Limitations during the TGA and Packed-Bed Experiments

Because of the high reactivity of the produced char, combined with the well-known high reaction heat of coal combustion reactions, it must be checked very carefully that the temperature of the char particle is not increased during combustion. Therefore, the experimental investigations, already discussed in section 4, were supported by theoretical calculations which are presented below.

The maximum amount of heat generated by the combustion reaction for a single particle $\phi_{max,reaction}$ (J/s) can be calculated with

$$\phi_{max,reaction} = V_p \rho_{char} \Delta H_r r_{max} \quad \text{(A1)}$$

in which V_p represents the volume of a particle (m^3), ρ_{char} the char density (kg/m^3), ΔH_r theheat of reaction (J/kg), and r_{max} the maximum reaction rate (s^{-1}). The amount of heat which can be transferred to the surrounding gas phase equals

$$\phi_{max,transfer} = \alpha A_p (T_p - T_{gas}) \quad \text{(A2)}$$

in which α represents the external heat-transfer coefficient (W/(m^2/K)), A_p represents the particle surface (m^2), and T_p and T_{gas} represent the particle temperature and gas temperature (K), respectively. When the amount of heat which is generated by the reaction is higher than the amount which can be transferred to the surrounding gas phase, the particle temperature will increase until a heat balance is reached

$$\phi_{max,reaction} = \phi_{max,transfer} \quad \text{(A3)}$$

The temperature increase ΔT will enhance the reaction rate constant, with respect to the reaction rate T_{gas} to

$$r_{max} = k_0 e^{-[E_a/R(T_{gas}+\Delta T)]} P_{O_2}{}^n \quad \text{(A4)}$$

By combination of (A1)−(A4), the following (implicit) equation can be derived for the temperature increase of the particle surface:

$$\Delta T = \frac{V_p \rho_{char} \Delta H_r k_0 e^{-[E_a/R(T_{gas}+\Delta T)]} P_{O_2}{}^n}{\alpha A_p} \quad \text{(A5)}$$

By linearization of the exponential term, which is allowed for small values of ΔT (with respect to T_{gas}):

$$e^{-[E_a/R(T_{gas}+\Delta T)]} \approx e^{-E_a/RT_{gas}} \left(1 - \frac{E_a}{RT_{gas}{}^2} \Delta T\right) \quad \text{(A6)}$$

the following explicit equation for ΔT can be derived:

$$\Delta T = \frac{\dfrac{V_p \rho_{char} \Delta H_r k_0 e^{-E_a/RT_{gas}} P_{O_2}{}^n}{\alpha A_p}}{1 + \dfrac{E_a V_p \rho_{char} \Delta H_r k_0 e^{-E_a/RT_{gas}} P_{O_2}{}^n}{RT^2_{gas} \alpha A_p}} \quad \text{(A7)}$$

Table 10 presents the values for the input parameters such as the maximum reaction rates, heat of reaction, characteristic particle diameter, char bulk density, and required physical properties of air. The external heat-transfer coefficient was experimentally determined in the TGA by recording the heat-up time of an (empty) basket, which yielded a value of 40 W/(m^2/K). In that case, the particle surface in (A7) should be replaced by the heat-transfer surface area of the basket (i.e., the bottom side of the basket with a diameter of 0.01 m). Here, the assumption is implicitly made that the particle temperature equals the temperature of the basket. Apart from a calculation for the heat transfer from the basket to the gas flow through the TGA tube, a second analysis has been carried out in which the heat transfer from the sample particles to the gas flow has been calculated on the basis of Nu ($=\alpha d_p/\lambda_{air}$) = 2, which yields a value of a of 1000 W/(m^2/K) (TGA) and 2000 W/(m^2/K) (packed bed). This approach makes sense

Table 10. Data for Heat-Transfer Limitation Calculation

		source
d_p (m)	10^{-4}	this work
E_A (kJ/mol)	125	this work
ρ_{char} (kg/m^3)	300	*a*
ΔH (MJ/kg)	30	*b*
α (TGA) (W/(m/K))	40	this work
α (TGA) (W/(m/K))	1000	$Nu = 2$
α (packed bed) (W/(m/K))	2000	*c*
r_{max} (450 °C, TGA) (1/s)	0.0269	this work (experiment)
r_{max} (500 °C, PB) (1/s)	0.1139	this work (experiment)
λ_{air} (500 °C) (W/(m/K))	0.05	*d*
Pr_{air} (500 °C)	0.69	*d*

[a] di Blasi (1993). [b] Bridgwater and Bridge (1991). [c] Gunn (1978). [d] Janssen and Warmoeskerken (1987).

Table 11. Temperature Difference between the Particle and Gas Phase

	temp difference ΔT (K)
TGA ($\alpha = 40$ W/(m/K), $A = A_{basket}$)	0.04
TGA ($\alpha = 1000$ W/(m/K), $A = A_p$)	3.6
packed bed	6.8

because the char particles in the TGA sample basket form a layer of at most one particle diameter thickness, while the char particles in the packed bed are diluted with the packing material alumina (1:1000). The result of the calculation, expressed in a temperature difference between the particle and gas phase, is presented in Table 11.

The experimentally determined value of the temperature difference in the TGA (3 K) is close to the theoretical calculation based on the $Nu = 2$ approach (3.6 K). For the packed bed, it can be expected also that the heat transfer is underestimated because of the high, thermal conductivity of the packing material alumina. Moreover, the overall heating of the gas phase could be neglected. This was established by the temperature profiles as observed in the axial and radial directions with the movable thermocouple in the bed (section 4). The conclusion is justified that the temperature increase of the sample was suppressed successfully in the two types of experimental equipments.

Literature Cited

Bhatia, S. K.; Perlmutter, D. D. A random pore model for fluid-solid reactions: I. isothermal, kinetic control. *AIChE J.* **1980**, *26*, 379.

Bridgwater, A. V.; Bridge, S. A. A Review of Biomass Pyrolysis and Pyrolysis Technologies. *Biomass Pyrolysis Liquids Upgrading and Utilisation*; Elsevier Science Publishing Co.: New York, 1991.

Brown, T. C.; Lear, A. E.; Haynes, B. S. Oxygen chemisorption on carbon. 24th Symposium on coal combustion, Chicago, 1992; p 1199.

Burggraaf, R.; Prins, W. Reaction kinetics of graphite and wood char. Unpublished results, Twente University, 1983.

Di Blasi, C. Analysis of convection and secondary reaction effects within porous solid fuels undergoing pyrolysis. *Combust. Sci. Technol.* **1993**, *90*, 315.

Floess, J. K.; Longwell, J. P.; Sarofim, A. F. Intrinsic reaction kinetics of microporous carbons. 1: Noncatalyzed chars. *Energy Fuels* **1988**, *2*, 18.

Gavalas, G. R. A random capillary model with application to char gasification at chemically controlled rates. *AIChE J.* **1980**, *26*, 577.

Graham, R. G.; Freel, B. A.; Bergougnou, M. A. The production of pyrolytic liquids, gas and char from wood and cellulose by fast pyrolysis. *Proceedings in Research in Thermochemical Biomass Conversion*; Bridgwater, A. V.; Kuester, J. L., Eds.; Elsevier Applied Science: New York, 1988; p 629.

Gunn, D. J. Transfer of heat or mass to particles in fixed and fluidised beds. *Int. J. Heat Mass Transfer* **1978**, *21*, 467.

Hindmarsh, C. J.; Thomas, K. M.; Wang, W. X.; Cai, H. Y.; Güel, A. J.; Dugwell, D. R.; Kandiyoti, R. A comparison of the pyrolysis of coal in wire-mesh and entrained flow reactors. *Fuel* **1995**, *74*, 1185.

Ismail, I. M. K.; Walker, P. L. Detection of low temperature carbon gasification using DSC and TGA. *Carbon* **1989**, *27*, 549.

Janse, A. M. C.; Prins, W.; van Swaaij, W. P. M. Development of a small integrated pilot plant for flash pyrolysis of biomass. In *Proceedings in Developments in Thermochemical Biomass Conversion*; Bridgwater, A.V., Boocock, D. G. B., Eds.; Blackie Academic and Professional: London, 1996; p 368.

Janssen, L. P. B. M.; Warmoeskerken, M. M. C. G. *Tranport phenomena data companion*; Delftse Uitgevers Maatschappij: Delft, The Netherlands, 1987.

Jenkins, R. G.; Nandi, S. P.; Walker, P. L., Jr. Reactivity of heat-treated coals in air at 500 °C. *Fuel* **1973**, *52*, 288.

Kashiwagi, T.; Nambu, H. Global kinetic constants for thermal oxidative degradation of a cellulosic paper. *Combust. Flame* **1992**, *88*, 345.

Kristiansen, A. *Understanding coal gasification*; IEA Coal Research: London, 1995.

Laurendeau, N. M. Heterogeneous kinetics of coal char gasification and combustion. *Prog. Energy Sci.* **1978**, *4*, 221.

Lin, L. C.; Deo, M. D.; Hanson, F. V.; Oblad, A. G. Non-isothermal analysis of the kinetics of the combustion of coked Sand. *Ind. Eng. Chem. Res.* **1991**, *30*, 1795.

Magnaterra, M. R.; Cukierman, A. L.; Lemcoff, N. O. Kinetic study of combustion of cellulose and a hardwood species char. *Lat Am. Appl. Res.* **1989**, *19*, 61.

Magnaterra, M. R.; Fusco, J. R.; Ochoa, J.; Cukierman, A. L. Kinetic study of the reaction of different hardwood sawdust char with oxygen. Chemical and structural characterization of the samples. In *Proceedings in Advances in thermochemical biomass conversion*; Bridgwater, A.V., Ed.; Blackie Academic and Professional: London, 1992; p 116.

McCarthy, D. J. Changes in oxyreactivity of carbons due to heat treatment and prehydrogenation. *Carbon* **1981**, *19*, 297.

McDonald, K. M.; Hyde, W. D.; Hecker, W. C. Low temperature char oxidation kinetics: effect of preparation method. *Fuel* **1992**, *71*, 319.

Miura, K.; Hashimoto, K.; Silveston, P. L. Factors affecting the reactivity of coal chars during gasification and indices representing reactivity. *Fuel* **1989**, *68*, 1461.

Patel, M. M.; Grow, D. T.; Young, B. C. Combustion rates of lignite char by TGA. *Fuel* **1988**, *67*, 165.

Prins, W. Fluidized bed combustion of a single carbon particle. Ph.D. Thesis, University of Twente, Enschede, The Netherlands, 1987.

Radovic, C. R.; Walker, P. L., Jr.; Jenkins, R. G. Importance of carbon active sites in the gasification of coal chars. *Fuel* **1983**, *62*, 849.

Scott, D. S.; Piskorz, J. The flash pyrolysis of aspen poplar wood. *Can. J. Chem. Eng.* **1982**, *60*, 666.

Shevchenko, A. O.; Ivakhnyuk, G. K.; Fedorov, N. F. Effect of electric current frequency on the activations kinetics of raw charcoal. *Russ. J Appl. Chem.* **1993**, *66*, 1109.

Simons, G. A.; Finson, M. L. The structure of coal char: Part I. Pore branching. *Combust. Sci. Technol.* **1979**, *19*, 217.

Tseng, H. P.; Edgar, T. F. The combustion behaviour of bituminous and anthracite coal between 425 and 900 °C. *Fuel* **1985**, *64*, 373.

Tseng, H. P.; Edgar, T. F. The change of physical properties of coal char during reaction. *Fuel* **1989**, *68*, 114.

Wagenaar, B. M.; Prins, W.; van Swaaij, W. P. M. Pyrolysis of biomass in the rotating cone reactor. *Chem. Eng. Sci.* **1994**, *49*, 5109.

Weeda, M. Kinetics of coal gasification under industrial conditions. Ph.D. Thesis, University of Amsterdam, Amsterdam, The Netherlands, 1995.

Westerhout, R. W. J.; Balk, R. H. P.; Meijer, R.; Kuipers, J. A. M.; van Swaaij, W. P. M. Measurement and modelling of the high temperature pyrolysis kinetics of polyethene and polypropene—application of a novel screen heater with a gas sweep. *Ind. Chem. Eng. Res.* **1998**, *36*, 3360−3368.

Wigmans, T.; Cranenburgh, H.; Elfring, R.; Moulijn, J. A. Mass transfer phenomena during potassium carbonate catalysed carbon steam gasification reactions in a microbalance set-up. *Carbon* **1983**, *21*, 23.

Zygourakis, K. The effects of pyrolysis conditions on the macropore structure of coal chars. *Prepr. Pap.—Am. Chem. Soc., Div. Fuel Chem.* **1988**, *33*, 951.

Received for review October 6, 1997
Revised manuscript received July 9, 1998
Accepted July 20, 1998

IE970705I